THE JOURNAL OF PHYSICAL CHEMISTRY B

ARTICLE

pubs.acs.org/JPCB

How Liposomes Diffuse in Concentrated Liposome Suspensions

Yan Yu,[†] Stephen M. Anthony,[‡] Sung Chul Bae,[†] and Steve Granick*[,†,‡,§]

Departments of [†]Materials Science and Engineering, [‡]Chemistry, and [§]Physics, University of Illinois, Urbana, Illinois 61801, United States

ABSTRACT: Building upon the observation that liposomes of zwitterionic lipids can be stabilized against fusion by the adsorption of cationic nanoparticles (Yu, Y.; Anthony, S.; Zhang, L.; Bae, S. C.; Granick, S. *J. Phys. Chem. C* **2007**, *111*, 8233), we study, using single-particle fluorescence tracking, mobility in this distinctively deformable colloid system, in the volume fraction range of $\varphi = 0.01$ to 0.7. Liposome motion is diffusive and homogeneous at low volume fractions, but separable fast and slow populations emerge as the volume fraction increases beyond $\varphi \approx 0.45$, the same volume fraction at which hard colloids with sufficiently strong attraction are known to experience gelation. This is reflected not only in scaling of the mean square displacement, but also in the step size distribution (van Hove function) measured by fluorescence imaging. The fast liposomes are observed to follow Brownian motion, and the slow ones follow anomalous diffusion characterized by a 1/3 time scaling of their mean square displacement.

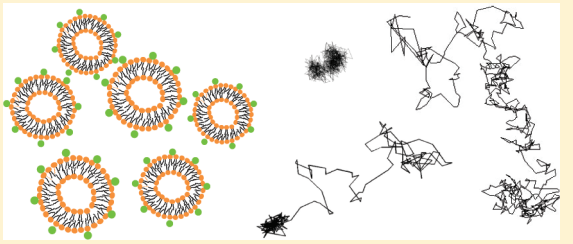

INTRODUCTION

A liposome is a droplet of fluid encapsulated by a phospholipid bilayer membrane formed by lipid self-assembly. As a simple model to mimic the cell membrane, liposomes have been widely used as carriers for gene transfection and drug delivery. Concentrated liposomes have also been used to mimic the heterogeneous and crowded environments inside cellular compartments in studies of the crowding effect on protein mobility.[1] Despite extensive studies of various applications of liposomes, understanding their physical properties such as rheology and dynamics remains a significant challenge, mainly due to their complexity. Much attention has focused on understanding the rheological properties of single liposomes in shear flow,[2,3] as well as liposome aggregation and fusion.[4−6] A few studies have investigated electrostatic and hydrodynamic effects on liposome diffusion in buffer or biopolymer solutions.[7−9] However, the dynamics of liposomes, especially in their concentrated forms, are largely unclear.

Dynamics in crowded environment can be difficult to predict because they depend on the solute size, charge, concentration, and complex interaction with solvent. In the most simplified cases where spherical colloidal particles interact with each other via hard-wall interactions, dynamics of the hard spheres are controlled by volume fraction. They change from simple Brownian motion in dilute solutions to anomalous diffusion at high volume fractions approaching the glass transition. In the jammed state, particles are dynamically arrested in transient cages formed by the surrounding particles and are only allowed to move over large distances during the rare and collective rearrangement of the cages.[10−12]Although in dilute solutions soft colloids such as liposomes are found to behave similarly to hard spheres,[8,13] their dynamical properties are expected to deviate in nontrivial ways because of the additional soft repulsions introduced by the deformability at volume fractions beyond random close packing of hard spheres. Studies on concentrated deformable microgels have observed spatial dynamical heterogeneities characterized by well separated regions of distinct dynamical activities and found that the heterogeneous dynamics are governed by clusters of particles undergoing irreversible rearrangements.[14,15] Other studies have also found that softness of the particles results in higher concentration for dynamical arrest and more gradual approach to the glass transition.[16,17] Many questions remain unclear, however, such as the structural origin of the dynamical heterogeneities and effects of softness on the dynamics. More importantly, do liposomes, as other types of deformable colloids such as microgels, behave differently in dense suspensions?

In this work, we study dynamics of concentrated liposomes and explore the roles of polydispersity and softness. Compared to conventional hard spheres with diameters of a few micrometers, liposomes studied here are more than an order of magnitude smaller, soft, and polydisperse. Unlike soft particles such as star polymers or pastes, fluorescent liposome tracers can be easily prepared by incorporating dye-labeled lipids into the bilayer membrane, allowing studies at single-liposome resolution using fluorescence imaging techniques. To keep the liposomes from fusion at high concentrations, small charged nanoparticles are allowed to adsorb on the lipid membrane, owing to the weak charge−dipole attraction between the nanoparticles and lipid dipolar headgroups, as we have demonstrated.[18,19] When liposomes are covered by the positively charged nanoparticles at ∼25% surface coverage, they remain discrete and exhibit Brownian motion at volume fractions up to 0.45.[16] In this study we find that, at higher concentrations, liposome dynamics become heterogeneous. The fast subpopulation is diffusive, but the

Received: September 24, 2010
Revised: January 19, 2011
Published: March 08, 2011

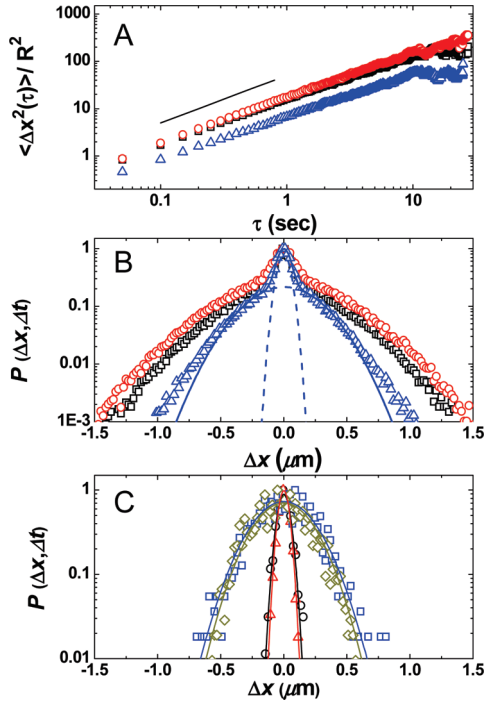

Figure 1. (A) Ensemble average mean-square displacement $\langle \Delta x^2(\tau) \rangle$, scaled to the square of the liposome hydrodynamic radius, R = 100 nm, plotted versus lag time τ for volume fractions φ = 0.53 (circles), φ = 0.57 (squares), and φ = 0.70 (triangles). The straight line indicates a slope of unity. (B) Displacement probability distribution $P(\Delta x, \Delta t)$ with a lag time Δt = 1 s for φ = 0.53 (circles), φ = 0.57 (squares), and φ = 0.70 (triangles). The solid line represents bimodal Gaussian fitting to the distribution for φ = 0.70, and the dashed lines indicate its two components. (C) $P(\Delta x, \Delta t)$ of four single liposomes with a lag time Δt = 1 s for φ = 0.70, each fitted with a single Gaussian function indicated by the solid lines. The number of steps averaged in each $P(\Delta x, \Delta t)$ is about 100 000 and about 2000 for the ensemble-average and single liposomes, respectively.

slower one diffuses anomalously. The heteronegeous dynamics of dense liposomes are surprisingly similar to the observations in softly repulsive colloids close to gelation, and structural heterogeneity is found to be the origin. We suggest the reason is a short-range attraction owing to the slight tendency of adsorbed nanoparticles to bridge between liposomes, combined with long-range electrostatic repulsion.

MATERIALS AND METHODS

Phospholipid 1,2-dilauroyl-*sn*-glycero-3-phosphocholine (DLPC) and the fluorescent lipid 1,2-dimyristoyl-*sn*-glycero-3-phosphoethanolamine (DMPE-RhB) were obtained from Avanti Polar Lipids, Inc. (Alabaster, AL). Positively charged aliphatic amidine polystyrene (PS) latex (diameter: 20 nm) with a charge density quoted by the manufacturer of 5.6 nm^2 per unit charge was purchased from Interfacial Dynamics Corp (Eugene, OR).

Liposomes comprised of DLPC with a diameter of 200 nm were prepared in deionized water (Millipore) using extrusion. Using quasi-elastic light scattering, we estimated the ratio of standard deviation to lipid vesicle diameter as 0.34. Liposomes were mixed with positively charged amidine PS nanoparticles at a molar ratio of 1:100, corresponding to ~25% surface coverage, or ~10% of total liposome volume. To ensure fluorescence imaging and accurate tracking at the single liposome level, liposome tracers with 0.1 mol % fluorescent lipid DMPE-RhB doped in the lipid bilayer were added to the stabilized liposome solution at a ratio of 1 tracer to 10^4 unlabeled liposomes, corresponding to approximately 1 per 80 μm^3. To quantify the effective volume fraction φ of the deformable liposomes, we used $\varphi = nV_0$, in which n is the number density of liposomes and $V_0 = 4\pi R^3/3$ is the volume of a liposome of radius R measured in dilute suspension, assuming no deformation. In all cases, the mixture was first prepared at φ = 0.01, then condensed by bubbling nitrogen gas gently over the suspension. Final concentrations were determined based on the known lipid amount and the sample volume. For imaging, a home-built epi-fluorescence microscope was employed. Dense liposome suspensions were kept in a sealed sample cell and allowed to equilibrate for 24 h prior to imaging. We focused about 3 μm away from the coverslip to avoid wall effects. Fluorescent liposomes were tracked using a modified implementation of standard single particle tracking algorithms described previously,[20,21] with a spatial resolution of ~50 nm. A total of approximately 300 liposome tracers were analyzed for each φ, resulting in ~300 trajectories, each of which lasts 50 steps or longer.

RESULTS AND DISCUSSION

In this study we use liposomes with an average diameter of 200 nm and positively charged nanoparticles of 20 nm. We first studied the ensemble average mean-square displacements, $\langle \Delta x^2(\tau) \rangle = \langle |x(t+\tau) - x(t)|^2 \rangle$, as a function of lag time τ for various volume fractions. The $\langle \Delta x^2(\tau) \rangle$, scaled to the square of the liposome hydrodynamic radius, all appear linear with τ for φ = 0.53, 0.57, and 0.70, as shown in Figure 1A, suggesting an overall diffusive behavior of the liposome tracers regardless of the high concentrations. While an ensemble average $\langle \Delta x^2(\tau) \rangle$ versus τ can reveal useful information in a homogeneous solution, it is prone to conceal dynamical heterogeneities. In contrast, the displacement probability distribution $P(\Delta x,\Delta t)$, the probability that a given liposome undergoes a displacement Δx along the x-axis within a time interval of duration Δt (also known as the van Hove distribution), provides a more discriminating measure of uniformity. For a simple random walk, $P(\Delta x,\Delta t)$ is a single-Gaussian distribution, and the variance of the distribution provides a measure of the diffusion coefficient. However, in glassy materials where particle motion is constrained, $P(\Delta x,\Delta t)$ develops substantial weight in the large-displacement wings. In Figure 1B, we plot $P(\Delta x,\Delta t)$ with a lag time Δt = 1 s against displacement Δx for φ = 0.53, 0.57, and 0.70 individually. One can see that all three plots deviate significantly from a single-Gaussian distribution, indicating a mobility different from the random walk suggested by the ensemble average mean-square displacement. In fact, each distribution can be fitted well by a sum of two Gaussian components, suggesting the existence of two distinct types of motion, one faster than the other. For visual clarity, only the bimodal fitting for φ = 0.70 is shown in Figure 1B. The bimodal distribution suggests several possibilities: one is that all liposomes are indistinguishable in motion but each acquires heterogeneous dynamics at different times; the second is that there are two distinct subpopulations of liposomes, either mobile or immobile; the third possibility is a combination of both.

To elucidate the origin, we examined $P(\Delta x,\Delta t)$ at the single liposome level. The $P(\Delta x,\Delta t)$ with a lag time Δt = 1 s of four representative liposomes at φ = 0.70 are plotted in Figure 1C. In

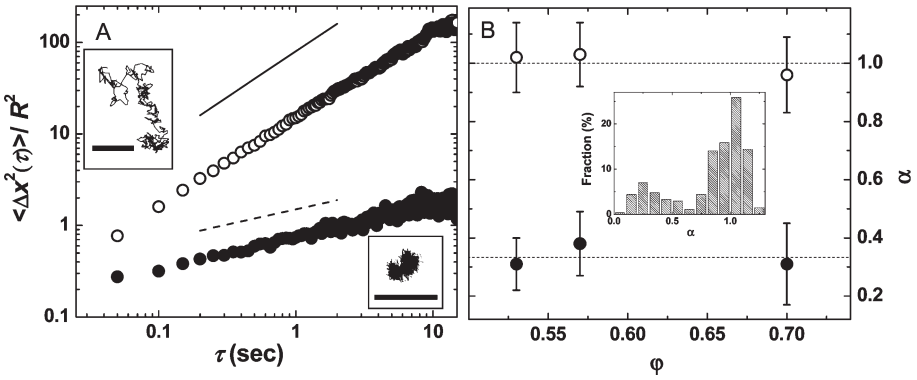

Figure 2. (A) Mean-square displacement $\langle \Delta x^2(\tau) \rangle$, scaled to the square of the liposome hydrodynamic radius R = 100 nm, of the fast (open symbols) and the slow (filled symbols) liposomes at $\varphi = 0.70$. The solid and dotted lines indicate a slope of 1 and 1/3 in the logarithmic plot, respectively. The total number of liposome tracers assessed is ~75 and ~220 for the slow and fast populations, respectively. (Insets) Two typical trajectories of the fast and slow liposomes. Each time step is 50 ms, and the total length of each trajectory is approximately 30 s. Scale bars: 500 nm. (B) Average α from $\langle \Delta x^2(\tau) \rangle \sim \tau^{\alpha}$ for the fast (open symbols) and slow (filled symbols) subpopulations are plotted against φ. As a guide to the eye, dotted lines indicate $\alpha = 1$ and $\alpha = 1/3$, respectively. Error bars are standard deviations. (Insets) Distribution of α of all single liposomes for $\varphi = 0.70$ exhibits two peaks, corresponding to the two subpopulations. The width of both peaks corresponds well to the expected distribution due to uncertainty in computing α from individual trajectories of finite length.

spite of the inevitably scattered data, due to limited statistics from single liposomes, it is evident that all four displacement probability distributions have single Gaussian distributions, but with different widths, which match either of the two widths from the bimodal Gaussian fitting. It indicates that there are two groups of liposomes, one diffusing faster than the other, and that the bimodal Gaussian distribution of liposome displacements in Figure 1B is simply the sum of both. Similar conclusions were obtained for φ = 0.53 and 0.57. In Figure 1, the total number of steps averaged in each $P(\Delta x, \Delta t)$ is about 100 000 and about 2000 for the ensemble-average and single-liposomes, respectively

We identified the fast and slow subpopulations independently based on their distinct mobilities. A threshold was chosen for the amplitude of a particle's fluctuation around its average position, $s = [(1/n)\Sigma_{i=1}^{n}(x_i - \bar{x})^2]^{1/2}$, in which x_i is the position at each time. Liposomes with s larger than the threshold are defined as the fast subpopulation, and those with s smaller than the threshold are the slow group. We find that the two populations are so distinguishable in mobility that varying the threshold over a wide range does not alter the subpopulation identification. The displacement probability distribution $P(\Delta x,\Delta t)$ of each subpopulation reproduces the fast and slow component from the bimodal Gaussian fitting in Figure 1B, confirming the success of this identification method.

As liposomes are polydisperse in nature, we first studied whether the distinctly different mobilities of liposomes are simply a result of different sizes. In the first control experiments, we identified and compared the size distribution of fast and slow liposomes. Because the liposome tracers were prepared with the constant ratio of fluorescently labeled lipids (RhB-DMPE) to unlabeled lipids (DLPC), larger liposomes have more labeled lipids on their surface and thus stronger fluorescence intensity. Therefore, we analyzed the size distribution of fast and slow liposomes separately by measuring their fluorescence intensity at a single liposome level. Both populations possess nearly identical size distributions (average fluorescence intensity for each liposome per image is $(9.7 \pm 4.1) \times 10^4$ a.u. for fast liposomes versus $(8.7 \pm 3.9) \times 10^4$ a.u. for the slow ones), indicating that the fast and slow liposomes do not differ in size. In another control experiment where smaller liposome tracers (mean diameter of 100 nm) were used in the concentrated liposome suspension at φ = 0.70, the coexistence of fast and slow liposomes were likewise observed. Both control experiments show that different mobilities of fast and slow liposomes cannot be discriminated by size, but it remains an open question whether polydispersity of the matrix (an unavoidable element of these experiments, as to prepare monodisperse liposomes is not possible technically) plays an essential role.

By plotting single liposome trajectories (insets in Figure 2A), we notice that the fast liposomes diffuse over distances several orders of magnitude larger than their own size, while the slow liposomes exhibit locally confined motion within a distance comparable to their own size, a feature similar to caging in hard sphere colloidal glasses.[6] To further explore the different diffusional behavior of the two populations, mean-square displacement $\langle \Delta x^2(\tau) \rangle$ of the fast and slow liposomes are plotted separately, and the results for $\varphi = 0.70$ are shown in Figure 2A. The $\langle \Delta x^2(\tau) \rangle$ of the fast liposomes is proportional to τ, as expected for a simple random walk. The mean diffusion coefficient, D = 0.033 $\mu m^2/s$, obtained by fitting $\langle \Delta x^2(\tau) \rangle$ with the equation for two-dimensional Brownian motion, $\langle \Delta x^2(\tau) \rangle = 4D\tau$, is nearly 30 times smaller than the diffusion coefficient of the same size liposomes in dilute solution ($D \approx 0.8-0.9\,\mu m^2/s$), likely due to the increased viscosity in the concentrated liposome suspensions. In contrast to the fast liposomes, the slow population diffuses anomalously, suggested by the nonlinear scaling: $\langle \Delta x^2(\tau) \rangle \sim \tau^{\alpha}$ with $\alpha \approx 1/3$. This power law is independent of the liposome concentrations, as shown in Figure 2B. For all three volume fractions φ = 0.53, 0.57, and 0.70, α of both liposome populations were found to be constant: $\alpha \approx 1$ for diffusive and $\approx 1/3$ for subdiffusive liposomes. The histogram of α obtained from single liposomes (the case of $\varphi = 0.70$ is shown in the inset of Figure 2B) confirms the same bimodal distribution. Moreover, the fractions of the two subpopulations obtained from the histograms are consistent with those obtained from the mobility identification method.

Further increasing the liposome concentration, we notice large dynamical changes. As shown in Figure 3A, despite the coexistence of diffusive and subdiffusive subpopulations for φ = 0.72,

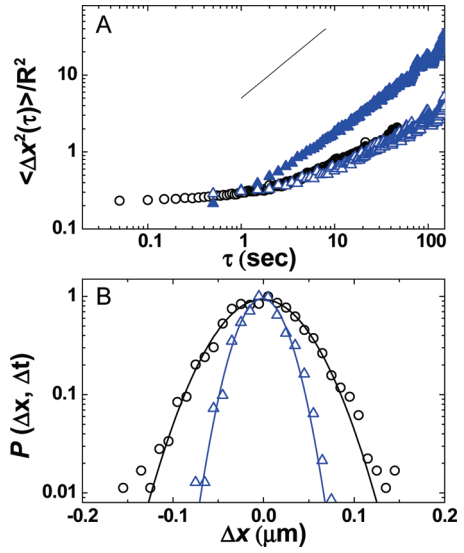

Figure 3. (A) Mean-square displacement $\langle \Delta x^2(\tau) \rangle$, scaled to the square of the liposome hydrodynamic radius R = 100 nm, of the fast (filled symbols) and the slow (open symbols) liposomes at φ = 0.72 (triangles) and φ = 0.73 (circles). No fast liposomes were observed for φ = 0.73. The solid line indicates a slope of 1 in the logarithmic plot. (B) P (Δx, Δt) of two single liposomes with a lag time Δt = 1 s for φ = 0.73, each fitted with a single Gaussian function indicated by the solid lines.

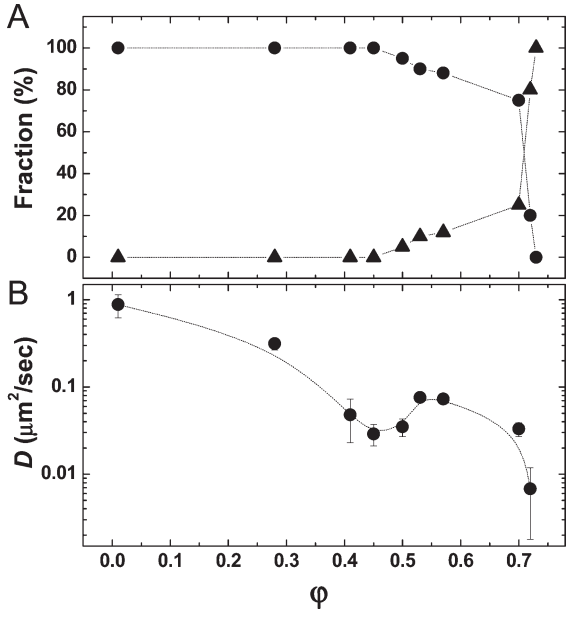

Figure 4. (A) Fractions of the fast (circles) and the slow (triangles) liposomes plotted versus φ. (B) Diffusion coefficient of the fast liposomes plotted against φ. Dotted lines are guides to the eye in both panels.

$\langle \Delta x^2(\tau) \rangle$ of the subdiffusive liposomes does not show the 1/3 scaling with lag time τ, but exhibits a plateau at shorter lag times, a feature reminiscent of arrested dynamics in glassy materials. A similar plateau in $\langle \Delta x^2(\tau) \rangle$ is also prominent for φ = 0.73, an extremely high concentration at which all liposomes were observed to be subdiffusive. Interesting, the displacement probability distribution $P(\Delta x,\Delta t)$ of individual liposome retains single-Gaussian distribution, as indicated in Figure 3B. The fraction

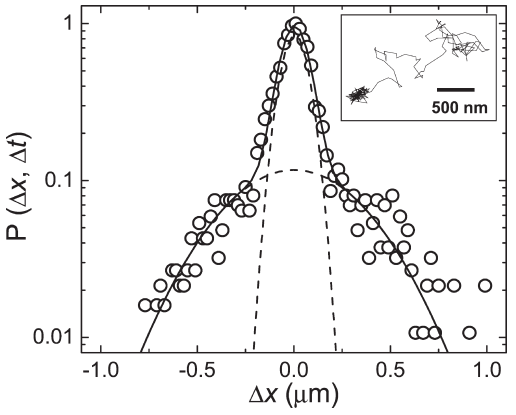

Figure 5. P (Δx, Δt) with a lag time Δt = 1 s of a typical "kiss-and-run" liposome at φ = 0.70 and its trajectory (inset). Each time step is 50 ms, and the total length of the trajectory is approximately 15 s.

of the two populations varies with φ, and so does the diffusion coefficient of the diffusive subpopulation, as shown in Figure 4. In dilute suspension (φ = 0.01), all liposomes are diffusive with an average diffusion coefficient of 0.8−0.9 $\mu m^2/s$. As concentration increases to φ = 0.45, dynamics remain homogeneous but slower by a factor of 30, a reflection of the increased viscosity in a more crowded environment. As φ increases beyond 0.45, separate fast and slow populations emerge. The slow liposomes start to diffuse anomalously and their abundance grows progressively at the expense of the fast subpopulation with an abrupt increase from φ = 0.70 to 0.72, followed immediately by the complete disappearance of diffusive liposomes at φ = 0.73. Surprisingly, the diffusion coefficient of the fast liposomes does not continuously decrease accordingly. They diffuse faster as φ increases from 0.45 to 0.53, indicating a lower *local* viscosity in spite of the elevated concentration.

The fact that this occurs at the same range of concentration over which the subdiffusive liposomes appear suggests a transition near φ = 0.45, akin to the spinodal decomposition observed in colloids with sufficiently strong attractions near gelation,[22,23] although the alternative explanation of flocculation cannot be excluded. This transition results in structural heterogeneities: regions of higher local liposome concentration where liposomes have anomalous diffusion due to the crowding, and regions of lower local concentration where there is still enough space for liposomes to move fast and diffusively. The driving force is possibly the short-ranged charge−dipole attraction of nanoparticles on one vesicle surface with adjacent vesicle surfaces at its nearest proximity, as our previous studies have found that liposomes can be bridged by nanoparticles at a lower surface coverage.[24] Our hypothesis of structural heterogeneity is supported by the existence of "kiss-and-run" liposomes, a very small fraction of liposomes (<0.5%) that were observed to switch between diffusive (fast) and subdiffusive (slow) behavior. As shown in Figure 5, the trajectory of one representative "kiss-and-run" liposomes resembles the features of both diffusive and dynamically arrested states, and its $P(\Delta x,\Delta t)$ with a lag time Δt = 1s clearly shows a bimodal Gaussian distribution. Such liposomes are believed to be located at the boundary between the regions of different densities. Their extremely low percentage and the fact that majority of the liposomes exhibit only either diffusive or subdiffusive motion during the entire experimental

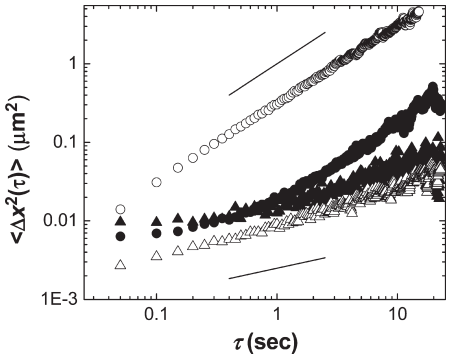

Figure 6. Mean-square displacements of the fast (filled circles) and the slow (filled triangles) tracer particles compared to those of the fast (open circles) and the slow (open triangles) liposomes both at $\varphi = 0.53$. The solid and dotted lines represent a slope of 1 and 1/3 in the logarithmic plot, respectively.

time window suggest that the exchange time between the two populations can be very long.

We further studied how the softness of liposome tracers affects their dynamics. The strategy was to replace liposome tracers, which are deformable, with monodisperse "hard" fluorescent particles (123 nm in diameter). The particles used in these control experiments had the same surface chemistry and similar charge density as the nanoparticles adsorbed on the liposome surfaces. Heterogeneous dynamics were also observed from single particle tracking: some particles diffuse over large distance, while others seem dynamically arrested. It suggests that the dynamical heterogeneity is not affected by softness of the tracer liposomes, but the matrix instead. Specifically, tracer particles were identified as either fast or slow using the same algorithm as described above, and their mean-square displacements are plotted and compared with those of liposome probes at the same concentration, $\varphi = 0.57$, in Figure 6. At time lags longer than 0.5 s, $\langle \Delta x^2(\tau) \rangle \sim \tau^{\alpha}$ with $\alpha \approx 1/3$ and $\alpha \approx 1$ for the fast and slow tracer particles, respectively, the same scaling as for the liposome probes. We notice that over long times, the slow components for both liposome tracers and hard particles diffuse a similar distance. However, at shorter time lags ($\tau < 0.5$ s), a plateau in the mean-square displacement occurs for the slow particles. This feature, absent from the liposome dynamics at the same concentration, only appears for more concentrated liposome suspensions (Figure 3A). It appears that soft tracer liposomes compared to hard particles are less likely to be jammed, consistent with studies reported elsewhere.[16] The responsible difference may be different softness. One possibility is that the softness of a particle affects its short-range diffusion, while the elastic response from surroundings determines its long-range dynamics. We now pay attention to the scaling law $\langle \Delta x^2(\tau) \rangle \sim \tau^{1/3}$, a scaling relation that persists from $\varphi = 0.53$ to 0.70 and emerges in the dynamics of both tracer particles and tracer liposome. Its robustness suggests that it arises from the physical nature of the dense liposomes. Transient anomalous diffusion described by $\langle \Delta x^2(\tau) \rangle \sim \tau^{\alpha}$ with $\alpha \approx 0.3-0.4$ has previously been observed in various systems, including hard sphere colloids under near-zero gravity, telomere diffusion inside the nucleus of mammalian cells, and proteins inside bacterial cytoplasm.[25−27] In the latter two studies, the presence of a viscoelastic environment is found to be the origin. The elasticity of the medium surrounding the particles creates long-time correlations in the particle's trajectories and subdiffusive behavior arises from the relaxation of Rouse modes.

To ascertain the extent to which concentrated liposome suspensions may be viscoelastic, we computed *local* viscous and elastic moduli from the single particle tracking results of the tracer particles using the one-particle microrheology formalism described in ref 28. The zero-shear viscosity is found to be 0.09 Pa·s for the fast particles at $\varphi = 0.57$. The G' and G'' can be well described by a Maxwell model with a single relaxation time implying a simply viscoelastic environment. However, it is very elastic locally around the slow particles, suggested by the elastic modulus G' dominating over the viscous modulus G'' at all times. When the same calculation was applied to a more concentrated liposome suspension, $\varphi = 0.73$, where all particle tracers are subdiffusive, the implied rheological response was nearly the same as that for the slow subpopulation at the lower volume fraction $\varphi = 0.57$. It is clear that increasing the global liposome concentration does not alter the microscopic elasticity of the regions with densely packed liposomes, but does change the size of such regions. This tends to confirm our hypothesis that structural heterogeneities in the concentrated liposome suspension lead to the heterogeneous dynamics, although this conclusion must be treated with caution since applicability of the microrheological formalism to heterogeneous systems is debatable.[29,30]

In conclusion, we presented a unique soft colloidal system comprised of polydisperse liposomes with charged nanoparticles adsorbed on their surfaces. With increasing concentration, a homogeneous liposome suspension becomes dynamically heterogeneous, in which liposome tracers are found to have different mobilities: the fast subpopulation has diffusive behavior while the slow subpopulation diffuses anomalously. The subdiffusional behavior characteristic of an $\alpha = 1/3$ power law in its mean-square displacement is attributed to the elastic medium surrounding the slow liposomes. At extremely high concentration when all liposomes appear subdiffusive, their dynamics resemble the features of caging phenomenon in hard spheres. Moreover, the fact that the fraction of slow liposomes grows at the expense of the fast liposomes as well as the striking increase of the fast liposome mobility at higher liposome concentration suggest that a spinodal-like transition results in heterogeneous structures microscopically and leads to the dynamical heterogeneity. With strong electrostatic repulsion and short-ranged attraction, dynamics of nanoparticle-stabilized liposomes in their dense suspensions are in surprising agreement with that of softly repulsive colloids approaching gelation.[22,31−34] As there is a short-ranged charge−dipole attraction between the positively charged nanoparticles and neutral liposomes, a possible driving force is the "bridging" between adjacent liposomes by the nanoparticles on their surfaces.

Even though dynamical heterogeneity has been studied in colloidal systems with short-ranged attraction both theoretically[31,32] and experimentally,[33,34] it has not been explored much in deformable colloids. Our study with the single-liposome tracking method allows us to explore the microscopic structure and its correlation with the dynamic heterogeneities in a system where objects are more than an order of magnitude smaller than traditional colloids. These results on the role of polydispersity and softness in dynamical heterogeneity can be significant to understand the dynamic and rheological problems of liposomes as well as other complex fluids. This study may also have implications for understanding diffusion in crowded biological environments, where the diffusing objects likewise are flexible and polydisperse.

AUTHOR INFORMATION

Corresponding Author
*E-mail address: sgranick@illinois.edu.

ACKNOWLEDGMENT

We thank Dr. Jacinta Conrad and Dr. Angelo Cacciuto for helpful discussion. This work was supported by the U.S. Department of Energy, Division of Materials Science, under Award No. DEFG02-02ER46019.

REFERENCES

(1) Engelke, H.; Dorn, I.; Radler, J. O. *Soft Matter* **2009**, *5*, 4283.
(2) Deschamps, J.; kanstler, V.; Steinberg, V. *Proc. Natl. Acad. Sci. U.S.A.* **2009**, *106*, 11444.
(3) Vlahovska, P. M.; Gracia, R. S. *Phys. Rev. E* **2007**, *75*, 016313.
(4) Raudino, A.; Pannuzzo, M. *J. Chem. Phys.* **2010**, *132*, 045103.
(5) Siegel, D. P. *Biophys. J.* **2008**, *95*, 5200.
(6) Roldan-Vargas, S.; Martin-Molina, A.; Quesada-Perez, M.; Barnadas-Rodriguez, R.; Estelrich, J.; Callejas-Fernandez, J. *Phys. Rev. E* **2007**, *75*, 021912.
(7) Rusu, L.; Lumma, D.; Radler, J. O. *Macromol. Biosci.* **2010**, *10*, 1465.
(8) Haro-Perez, C.; Quesada-Perez, M.; Callejas-Fernandez, J.; Casals, E.; Estelrich, J.; Hidalgo-Alvarez, R. *J. Chem. Phys.* **2003**, *119*, 628.
(9) Galera-Cortés, E.; Solier, J. d. D.; Estelrich, J.; Hidalgo-Álvarez, R. *Langmuir* **2010**, *26*, 2665.
(10) Pusey, P. N.; van Megen, W. *Nature* **1986**, *320*, 340.
(11) Weeks, E. R.; Crocker, J. C.; Levit, A. C.; Schofield, A.; Weitz, D. A. *Science* **2000**, *287*, 627.
(12) Weeks, E. R.; Weitz, D. A. *Phys. Rev. Lett.* **2002**, *89*, 095704.
(13) Buitanhuis, J.; Forster, S. *J. Chem. Phys.* **1997**, *107*, 262.
(14) Yunker, P.; Zhang, Z.; Aptowicz, K. B.; Yodh, A. G. *Phys. Rev. Lett.* **2009**, *103*, 115701.
(15) Sessoms, D. A.; Bischofberger, I.; Cipelletti, L.; Trappe, V. *Phil. Trans. R. Soc. A* **2009**, *367*, 5013.
(16) Purnomo, E. H.; van den Ende, D.; Vanapalli, S. A.; Mugele, F. *Phys. Rev. Lett.* **2008**, *101*, 238301.
(17) Mattson, J.; Wyss, H. M.; Fernandez-Nieves, A.; Miyazaki, K.; Hu, Z.; Reichman, D. R; Weitz, D. A. *Nature* **2009**, *462*, 83.
(18) Zhang, L.; Granick, S. *Nano Lett.* **2006**, *6*, 694.
(19) Yu, Y.; Anthony, S.; Zhang, L.; Bae, S. C.; Granick, S. *J. Phys. Chem. C* **2007**, *111*, 8233.
(20) Anthony, S.; Granick, S. *Langmuir* **2009**, *25*, 8152.
(21) Anthony, S.; Zhang, L.; Granick, S. *Langmuir* **2006**, *22*, 5266.
(22) Manley, S.; Wyss, H. M.; Miyazaki, K.; Conrad, J. C.; Trappe, V.; Kaufman, L. J.; Reichman, D. R.; Weitz, D. A. *Phys. Rev. Lett.* **2005**, *95*, 238302.
(23) Bailey, A. E.; Poon, W. C. K.; Christianson, R. J.; Schofield, A. B.; Gasser, U.; Prasad, V.; Manley, S.; Segre, P. N.; Cipelletti, L.; Meyer, W. V.; Doherty, M. P.; Sankaran, S.; Jankovsky, A. L.; Shiley, W. L.; Bowen, J. P.; Eggers, J. C.; Kurta, C.; Lorik, T.; Pusey, P. N.; Weitz, D. *Phys. Rev. Lett.* **2007**, *99*, 205701.
(24) Zhang, L.; Dammann, K.; Bae, S. C.; Granick, S. *Soft Matter* **2007**, *3*, 551.
(25) Simeonova, N. B.; Kegel, W. K. *Phys. Rev. Lett.* **2004**, *93*, 035701.
(26) Bronstein, I.; Israel, Y.; Kepten, E.; Mai, S.; Shav-Tal, Y.; Barkai, E.; Garini, Y. *Phys. Rev. Lett.* **2009**, *103*, 018102.
(27) Weber, S. C.; Spakowitz, A. J.; Theriot, J. A. *Phys. Rev. Lett.* **2010**, *104*, 238102.
(28) Mason, T. G.; Ganesan, K.; van Zanten, J. H.; Wirtz, D.; Kuo, S. C. *Phys. Rev. Lett.* **1997**, *79*, 3282.
(29) Gardel, M. L.; Valentine, M. T.; Crocker, J. C.; Bausch, A. R.; Weitz, D. A. *Phys. Rev. Lett.* **2003**, *91*, 158302.
(30) Liu, J.; Gardel, M. L.; Kroy, K.; Frey, E.; Hoffman, B. D.; Crocker, J. C.; Bausch, A. R.; Weitz, D. A. *Phys. Rev. Lett.* **2006**, *96*, 118104.
(31) Puertas, A. M.; Fuchs, M.; Cates, M. E. *J. Chem. Phys.* **2004**, *21*, 2813.
(32) Reichman, D. R.; Rabani, E.; Geissler, P. L. *J. Phys. Chem. B* **2005**, *109*, 14654.
(33) Gao, Y.; Kilfoil, M. L. *Phys. Rev. Lett.* **2007**, *99*, 078301.
(34) Dibble, C. J.; Kogan, M.; Solomon, M. J. *Phys. Rev. E* **2008**, *77*, 050401.